

Firing Properties of the Soma and Axon of the Abdominal Stretch Receptor Neurons in the Crayfish (*Astacus leptodactylus*)

N. PURALI

Hacettepe University, Medical Faculty, Department of Biophysics, Ankara, Turkey

Abstract. Action potentials (APs) and impulse responses in the soma and axon of the rapidly and slowly adapting (SA) abdominal stretch receptor neurons of the crayfish (*Astacus leptodactylus*) were recorded with single microelectrode current-clamp technique. Impulse frequency response to constant current injection was almost constant in the SA neuron while the response decayed completely in the rapidly adapting (RA) neuron. Mean impulse frequency responses to current stimulations were similar in the receptor neuron pairs. In the RA neuron additional current steps evoked additional impulses while a sudden drop in the current amplitude caused adaptation. Impulse duration was dependent on the rate of rise when current ramps were used. Adaptation was facilitated when calculated receptor current was used. Exposing the neuron to 3 mmol/l TEA or scorpion venom resulted in partly elongated impulse responses. SA neuron could continuously convert the current input into impulse frequency irrespective of previous stimulation conditions. Exposing the SA neuron to 3 mmol/l TEA or 1 mmol/l Lidocaine reduced impulse duration to large current stimulations. The SA neuron fired spontaneously if it was exposed to 5–10 mmol/l Lidocaine or 10^{-2} mg/ml *Leiurus quinquestriatus* venom. The action potential (AP) amplitudes in the RA soma, RA axon, SA soma, and SA axon were significantly different between components of all pairs. Duration of the AP in the axon of the RA neuron was significantly shorter than those in the RA soma, SA soma, and SA axon. Diameter of the RA axon was larger than that of the SA axon. Non-adapting impulse responses were promptly observed only in the SA axons. The results indicate that the RA neuron is a sort of rate receptor transducing the rapid length changes in the receptor muscle while the SA neuron is capable of transducing the maintained length changes in the receptor muscle. The differences in firing properties mainly originate from the differences in the active and passive properties of the receptor neurons.

Key words: Crayfish — Stretch receptor — Adaptation — Lidocaine — Scorpion venom

Correspondence to: Dr. Nuhan Purali, Hacettepe University, Medical Faculty, Department of Biophysics, 06100 Sıhhiye, Ankara, Turkey. E-mail: npurali@hacettepe.edu.tr

Introduction

Considering the number of the published articles, the abdominal stretch receptor organs of the crayfish are perhaps the most extensively studied mechanoreceptors since they were first described by Alexandrowitz (1951). Majority of the reported works on these primary receptors focused on the mechanisms of mechanotransduction or adaptation process. In this context, visco-elastic properties of the receptor muscles and the electrical properties of the receptor neurons have been investigated comparatively in the rapidly and slowly adapting (RA, SA) receptors (for review see Swerup and Rydqvist 1992; Purali 1997).

Both receptors are specifically involved in converting the mechanical stimulus into neural codes, conveying information to the abdominal ganglia. Features of the mechanical stimulus are represented in timing and frequency of the evoked impulse responses. Timing of the receptor responses has been investigated in several works (Nakajima and Onodera 1969; Fields 1976; Purali 1997) since the pioneer work by Wiersma et al. (1953). Reports are available about impulse frequency responses in the SA receptor neuron (Terzuolo and Washizu 1962; Brown and Stein 1966; Chaplain et al. 1971). However, properties of the RA neuron have been ignored. Presently, only few hand made frequency measurements at a certain moment of the stimulation are available (Nakajima and Onodera 1969; Rydqvist and Purali 1993). In the present study timing and firing frequency of the impulse responses to current stimulations in the RA and SA neurons have been investigated. In addition, effects of some chemicals altering the adaptation properties of the receptor neurons, have been investigated.

Experiments in all the former studies have been performed on neuronal soma due to the relative simplicity of experimentation as compared to that on the axon. In the present study firing properties of the RA and SA axons, at about 1–1.5 mm away from cell soma, are firstly investigated.

Recordings from the RA and SA neurons were analysed and the results were comparatively discussed to define the physiological task the receptor neurons were performing.

Materials and Methods

Preparations

The experiments were carried out on the RA and SA stretch receptors of the crayfish, *Astacus leptodactylus*. Experimental animals were collected in the lakes of Central Turkey and kept in an aerated aquarium at 18–20°C, on an alternating carrot and fish diet once a week. In the use of experimental animals the guidelines by Hacettepe University have been followed and ethics committee approval has been obtained. The stretch receptor pairs were dissected from the second to fourth abdominal segments of the crayfish and transported into a recording chamber. The chamber was placed onto an inverted microscope (TE Eclipse 200, Nikon, Japan).

Neuronal soma and axon were identified using interference contrast system of the microscope and a manipulator (MHW-3, Narishige, Japan) was used for positioning the intracellular recording microelectrode. Experiments were carried out at room temperature (20–22°C).

Solutions

Composition of the control solution was (in mmol/l) 200 NaCl, 5.4 KCl, 13.5 CaCl₂, 2.6 MgCl₂ (van Harreveld 1936) and buffered to pH 7.4 using 10 mmol/l HEPES (Sigma Chemical Co. St. Louis, USA). 3 mmol/l tetraethylammonium chloride (Sigma Chemical Co. St. Louis, USA) solution was prepared by substituting equivalent mol of NaCl in the control solution with tetraethylammonium. The proper chemicals were added to the control solution in order to obtain 1–10 mmol/l Lidocaine (Sigma Chemical Co. St. Louis, USA) or 10⁻² mg/ml *Leiurus quinquestriatus* venom (V-5251, Lot #37H0996, Sigma Chemical Co. St. Louis, USA).

Stimulation and recording

Glass microelectrodes were manufactured from glass capillary (GC150F, Clarke Electromedical Instruments, Reading, UK) in a vertical puller (700 C David Kopf Instruments, New York, USA). The electrodes (2–7 MΩ) were filled with 3 mol/l KCL solution. The reference electrode was an Ag/AgCl wire immersed in the bathing solution.

The recording apparatus, manufactured by myself, was a bridge circuit enabling potential recording and simultaneous current injection through a single electrode. The design principle was identical to the one reported elsewhere (Smith et al. 1985). The unity gain buffer amplifier was a TL071 (Texas Instruments, USA). The current injection was achieved by delivering a calibrated external potential signal *via* an OP07 (Texas Instruments, USA) through a 100 MΩ resistor to the recording electrode. The frequency band of the apparatus was improved by an adjustable negative capacitance correction circuit, as proposed by Smith et al. (1985). Signals from the main amplifier were corrected by bridge balance and electrode off set balance stages mainly using OP07 amplifiers and several variable resistors.

The stimulus waveform was generated in a personal computer and the signal from the recording apparatus was digitised and stored in the same computer. The software for stimulation and recording were programmed in our department. The sampling rate was 20 kHz for action potential and 10 kHz for impulse response recordings. Filtering of any type has not been used.

Epi-Fluorescent microscopy

The fluorescent dye Alexa 594 (Molecular Probes, USA) was loaded into the receptor neuron *via* a somal microelectrode. The dye diffused uniformly within the cell compartments. TE-FM epi-flouresence attachment in combination with a band pass filter Y-2E/C (Nikon, Japan) was used to observe the fluorescent image of the neurons in the microscope. Images were photographed by a camera (F-601/P-III, Nikon, Japan).

Digital solutions

In the present study two different digital interventions were used; firstly to measure the firing frequency in a recorded impulse response and secondly to empirically calculate an average receptor current.

An algorithm, calculating the firing frequency of a digitised impulse response, was developed in Matlab (The Math Works Inc., USA) environment. The program calculated the inverse value of the period between successive APs. Accordingly, frequency was calculated only if there were at least two APs and the calculated frequency was registered to the following AP in the pairs.

Timing of the APs was determined principally by digital differentiation and threshold implementation. Capacitative spikes, observed in some experiments were excluded by removing the first and/or the last element by activating some correction commands.

The receptor current from a ramp-and-hold extension was calculated according to the model proposed by Swerup and Rydqvist 1996. However, some parameters were changed, and the tension in the (RA) receptor muscle was calculated by digitally solving the non-linear differential equation (2) for ε_2 in Simulink section of the Matlab program.

Definitions and equations for calculation of the tension in the receptor muscle and the receptor current in the receptor neuron are listed below:

$$\sigma_m = k \cdot \varepsilon_2 = k_2 \cdot \varepsilon_2^{n+1} = k_1 \cdot \varepsilon_1 + B \cdot d\varepsilon_1/dt \quad (1)$$

$$d\varepsilon_2/dt + k_1 \cdot \varepsilon_2/B + k_2 \cdot \varepsilon_2^{n+1}/B = k_1 \cdot \varepsilon/B + d\varepsilon/dt \quad (2)$$

$$\sigma = \sigma_m/25$$

where ε is extension, t is time, α is rise rate of the ramp; ε_1 , ε_2 are extensions in the linear and non-linear springs; k_1 , k_2 , B are the constants for linear and non-linear springs and the dash-pot; k is the non-linear parameter for the non-linear spring; σ_m is the tension in the receptor muscle.

The open probability of the mechanosensitive channel population P_o was assumed to change as a function of the tension developed in the receptor muscle (Guharay and Sachs 1984) according to the equation below.

$$P_o = 1/[1 + 500 \cdot \exp(-\sigma \cdot 0.011)] \quad (3)$$

Finally, the receptor current I_r was calculated by multiplying the P_o by the experimentally observed maximum stretch induced current I_{\max} (200 nA) in the RA receptor neuron when voltage clamped at resting potential (Rydqvist and Purali 1993). Thus the final form of the equation giving the receptor current (in nA) was as follows

$$I_r = I_{\max} \cdot P_o = 200/[1 + 500 \cdot \exp(-\sigma \cdot 0.011)] \quad (4)$$

Statistical analysis

The results are expressed as means \pm standard error of the means (S.E.M). Depending on the purpose of the analysis various inferential statistical methods were used to define the statistical significance of the results. Grouped results were subjected to one-way ANOVA analysis. Fisher's protected *t*-test was used for multiple comparison of groups when one-way ANOVA test indicated a significant difference. The relation between the paired measurements was quantified by using correlation analysis or paired *t*-test. All statistical analyses were performed in Matlab environment either by using the available commands or by constructing a program for the equations described somewhere else (Carmer and Swanson 1973; Welowitz et al. 1982). $p < 0.05$ was considered statistically significant.

Results

Impulse responses

Current stimulations evoked impulse responses in the RA and SA neurons. The impulse frequency correlated with the stimulus amplitude in both the RA and SA neurons. Impulse duration in the RA neuron increased to a certain level by increasing the stimulus amplitude, and decreased when the stimulus amplitude was increased further (Fig. 1). The same stimulations evoked maintained impulse responses in the SA neuron, and adaptation was observed only when an unusually large (≥ 15 nA) and maintained current stimulation was used (Fig. 8).

In the SA neuron impulse frequency responses consisted of a fast initial peak which decayed rapidly to a slowly diminishing steady level. If the initial part of the stimulation was ignored, the frequency curve was almost flat. Amount of the maximal noise (0.66 ± 0.11 Hz) in the flat part of the frequency curve to 5 nA current injection was significantly lower than that obtained to 11 nA current injection (0.9 ± 0.06 Hz) ($n = 6$, $p = 0.013$). In the RA neuron, a hump was observed in the impulse frequency responses. The hump was apparent to large current stimulations and took place at the junction where the initial peak amplitude relaxed to a slowly decaying plateau. The decay of the frequency responses was complete and apparently faster in the RA neuron as compared to that observed in the SA neuron (Fig. 1).

In each side of an abdominal segment there is a pair of stretch receptors containing one RA and one SA receptor organ. In order to achieve a maximum similarity between the experiments, the stimulus response relations were extracted from the recordings in the RA and SA neurons of five receptor pairs (Fig. 2). The mean firing frequency and the number of action potentials in the evoked impulse responses to 2 seconds long current stimulations were fitted to the power function $f = a(S - S_o)^n$, defining the receptor response (Stevens 1957), where S is the current stimulus and S_o is the threshold stimulus. Residual variance (*rv*) of the iterative calculation at 95% confidence interval was used for comparison of the fit results.

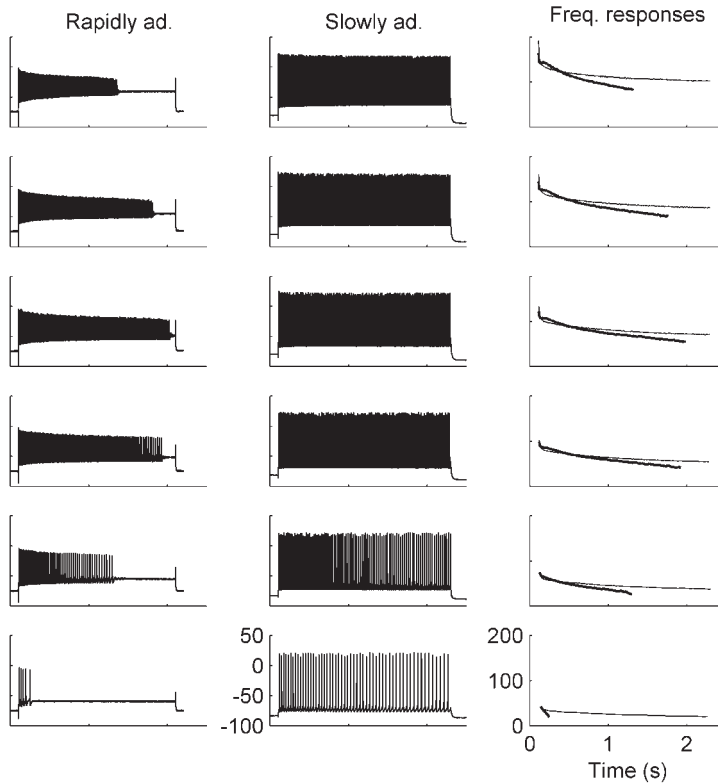


Figure 1. Receptor responses to constant current stimulations (from 3 to 13 nA in 2 nA increments, from bottom to top). Impulse responses in the rapidly (left column) and slowly (middle column) adapting neurons. Superimposed impulse frequency responses (right column) in the rapidly (thick line) and slowly (thin line) adapting neurons. Scales (in mV, Hz, s) are shown at the bottom.

The mean impulse frequency response had a similar behaviour in the both receptor neurons (Fig. 2A). Fit results of the experimental data were $a = 23.6$ Hz, $n = 0.576$, $rv = 0.0080$ in the SA neuron, and $a = 26.7$ Hz, $n = 0.556$, $rv = 0.0079$ in the RA neuron.

Stimulus-response relations from the RA and SA receptor neurons differed apparently when the number of APs in the evoked impulse trains was taken as the receptor response (Fig. 2B). The fit results of the experimental data were $a = 48$, $n = 0.570$, $rv = 0.0079$ in the SA neuron. In the RA neuron experimental data poorly fitted to the power function and the results were $a = 56.2$, $n = 0.457$, $rv = 0.0481$.

In the SA neuron, the rv increased only few percent by substituting the calculated parameters for the mean impulse frequency response with those for the

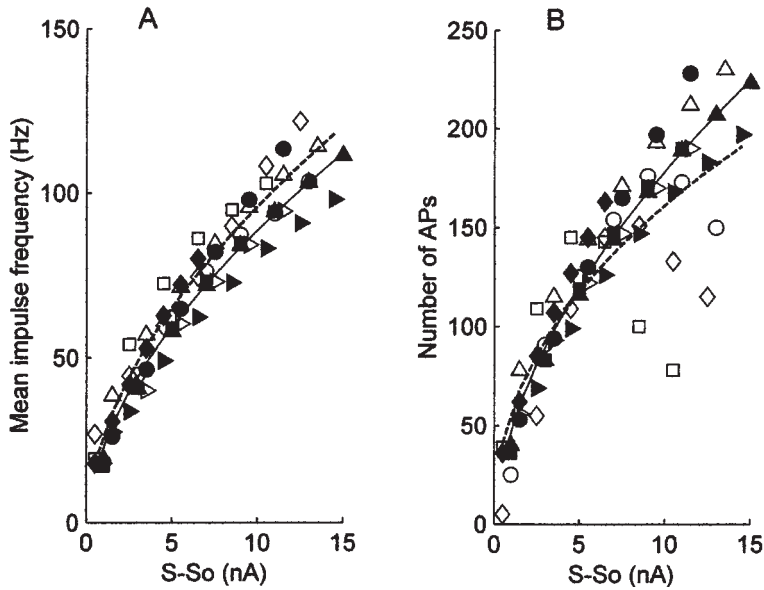


Figure 2. Comparison of the stimulus response relations obtained in the rapidly and slowly adapting neurons of five receptor pairs. Mean impulse frequency (A) and the number of action potentials (B) in the evoked impulse response is plotted against current stimulus (duration 2 s). Each receptor pair is represented by the same symbol in both graphs. The hollow and filled symbols are the rapidly and the slowly adapting neurons, respectively. The dotted and the solid lines are the fit results of the cumulative data to the power function, defining the receptor responses in the rapidly and slowly adapting neurons, respectively.

number of APs in the impulse response. However, such a change increased the rv to 0.0301 from 0.0079 in the RA neuron.

The RA neuron had a limited firing capacity. The capacity of the neuron was modulated by changing the waveform of the current stimulus. 5 nA constant current injection caused adaptation in many RA neurons within 2–3 seconds (cf. Figs. 1 and 2). However, additional current injections, *super pulses*, initiated AP or impulse responses (Fig. 3A). The RA cells responded to a sudden decrease in the stimulus amplitude by ceasing the impulse firing. Though the large and small constant current stimulations both evoked maintained impulse responses, the rapid transition from the large to small level caused adaptation (Fig. 3B). When current ramps were used, changing the rising rate of the ramp evoked a bimodal behaviour in impulse duration (Fig. 3C). An intermediate rise rate evoked the longest impulse train while adaptation was facilitated if faster or slower rise rates were used. Further, a very slowly rising ramp evoked a suprathreshold depolarisation but no AP. In contrast, the SA neuron fired whenever the threshold potential was achieved and this could not be manipulated by changing the stimulus waveform.

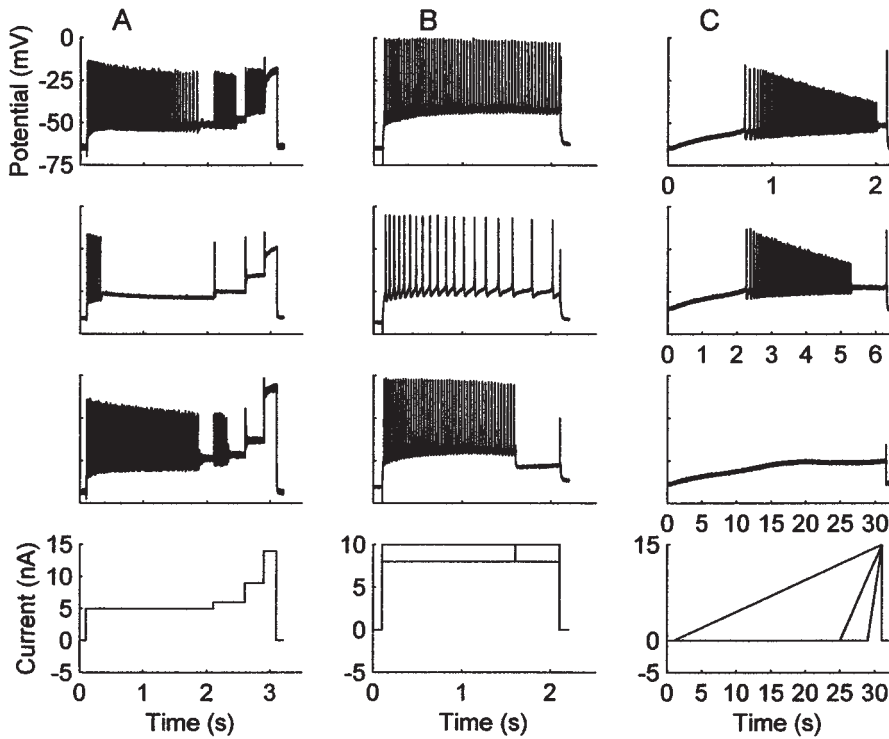


Figure 3. Potential responses to various current stimulations in the rapidly adapting neuron. In column A are the responses from three neurons to the current stimulus shown at the bottom. In column B there are the impulse responses to 10 and 8 nA constant current injection and the sudden stop of firing to an instantaneous transition of the stimulus from 10 to 8 nA, from top to bottom, respectively. Superimposed current stimulus waveforms are at the bottom. Potential responses to 15 nA current ramp at various ramp rise rates (0.5, 2.5, 7.5 nA s⁻¹ from bottom to top) are shown in column C. Potential scale is the same, and the time scales in A and B are as shown at the bottom. Notice the expanding time scales (in s) in C.

Firing properties of the RA neuron were investigated using a non-linear current stimulus simulating the receptor current to a ramp-and-hold extension. The tension, σ , in the receptor muscle to a 20% extension was calculated by solving equation (5) when $k_1 = 400$ kPa; $k_2 = 3200$ kPa; $B = 6$ kPa; $\alpha = 375\%$ s⁻¹. Receptor current, composed of a rapidly developing initial peak decaying to a constant plateau level, was calculated according to equations (3) and (4). Impulse frequency response to the calculated current stimulus increased during the ramp phase of stimulation and, decayed rapidly during the hold phase (Fig. 4A). The apparent decay observed during the hold period of an experimentally recorded receptor current (Rydqvist and Purali 1993) was absent in the calculated receptor

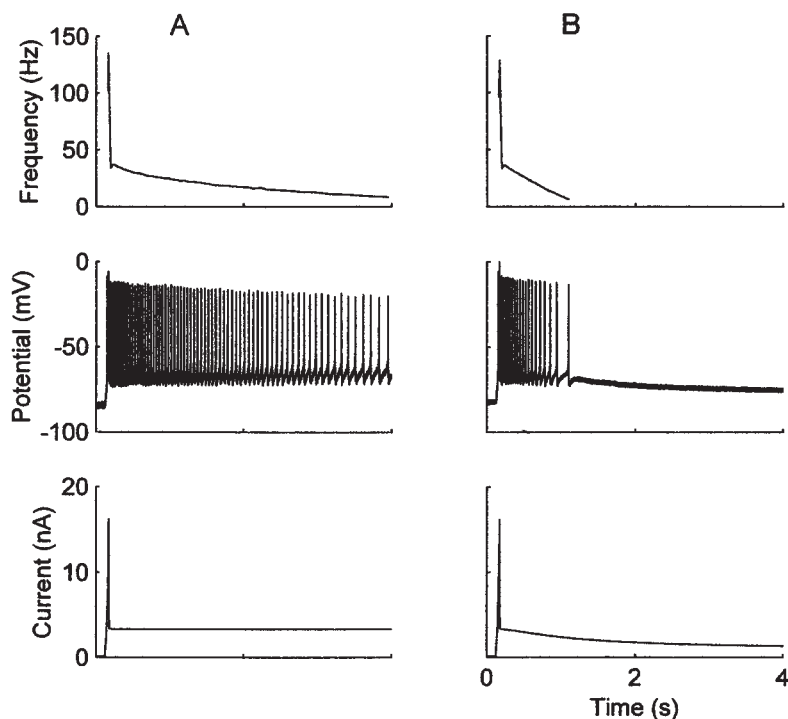


Figure 4. Receptor responses to calculated receptor currents to 20% extension in the rapidly adapting neuron. Impulse response (middle traces) and the impulse frequency response (top traces) to calculated nonadaptive (A), and adaptive (B) receptor currents (bottom traces). Time scale is the same for all graphs.

current (Fig. 4A). Thus, an exponential function was used to represent empirically the adaptation in the calculated tension response (Swerup and Rydqvist 1996). The function was activating simultaneously with the extension and capable of removing 25% of the maximal tension response with two time constants ($\tau_1 = 0.4$ s; $\tau_2 = 4$ s). Such an intervention led to similar values of the current calculated (Fig. 4B) and the one recorded experimentally (Rydqvist and Purali 1993). Initial part of the both calculations and the evoked responses were similar. However, impulse frequency to the adaptive current stimulus (Fig. 4B) was adapting more rapidly than that in the former experiment (Fig. 4A). Impulse responses during a cumulative stimulation were investigated using a calculated receptor current to successive extensions of 15, 20, 25%, respectively (Fig. 5). Onset of each extension level evoked impulses. The longest pulse train was observed at 20%, and the adaptation at 25% extension (Fig. 5A). The potential response to the same extension was apparently different when a calculated adaptive stimulus was used (Fig. 5B). The maximal firing rate was either the same or changing slightly within the extensions, and the longest

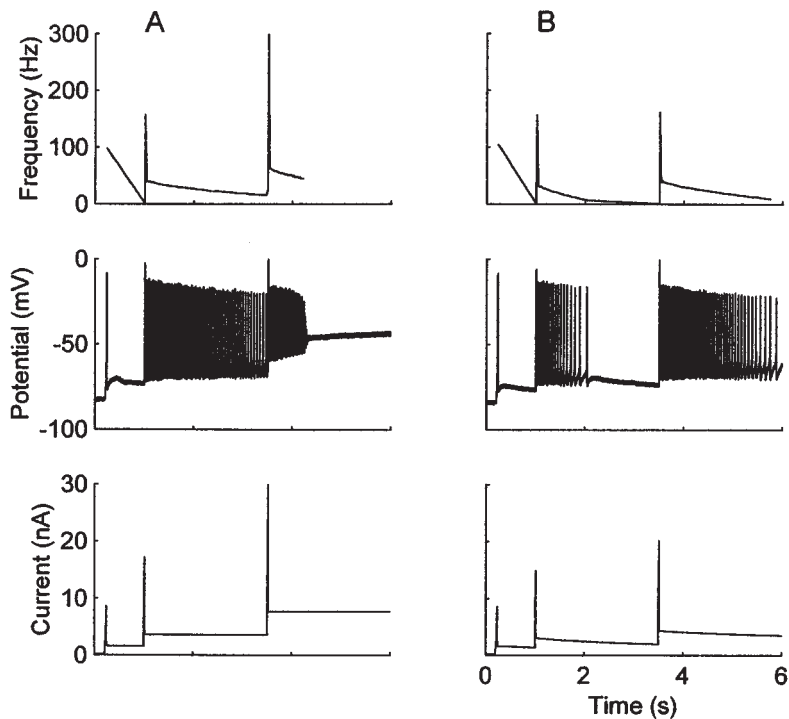


Figure 5. Receptor responses to calculated receptor currents to cumulative extensions to 15, 20, 25% in the rapidly adapting neuron. Impulse responses (middle traces) and the impulse frequency responses (top traces) to calculated nonadaptive (A), and adaptive (B) receptor currents (bottom traces). Time scale is the same for all graphs.

impulse response was obtained at 25% extension (Fig. 5B) where non-adapting current stimulus caused saturation (Fig. 5A). The hump (cf. Figs. 1 and 7) in the impulse frequency response was present in all recordings irrespective of stimulus waveform.

Some chemicals, modulating the gating properties of the potassium and the sodium channels, were experimented in the RA neuron. The cells were stimulated by 1–15 nA current injections (in 2 nA increments for 2.2 s) in: control, 3 mmol/l TEA, 1 mmol/l Lidocaine and 10^{-2} mg/ml *Leiurus quinquestriatus* venom solutions. In between the experiments the cells were washed in fresh control solution several times. Effects of TEA and Lidocaine were completely reversible. Results of a representative experiment have been shown in Fig. 6. TEA exposure increased the duration of impulse responses to current stimulations in the range of 1–7 nA. However, duration of the impulse response decreased when larger stimulations were used. Lidocaine exposure mainly reduced the duration of the impulse response but, an increase was observed if the stimulus amplitude was low (<5 nA). *Leiu-*

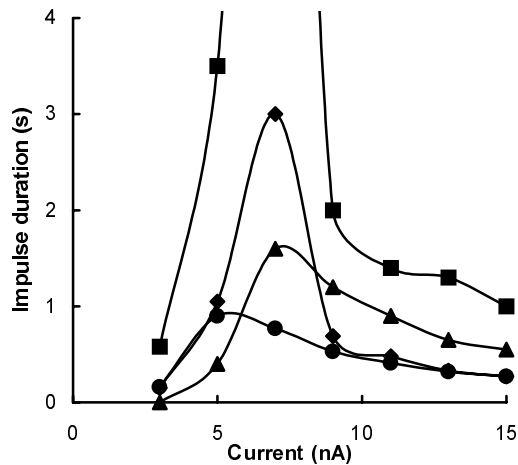


Figure 6. Effects of some chemicals on duration of impulse responses in a rapidly adapting neuron. Impulse duration *versus* injected current in control experiment (▲) and when the neuron was exposed to 3 mmol/l TEA (◆), 1 mmol/l Lidocaine (●) or 10^{-2} mg/ml *Leiurus quinquestriatus* venom (■).

rus quinquestriatus venom exposure increased duration of the impulse response at all stimulation levels and, initiated a non-adapting impulse response to 7 nA current stimulus. Firing frequencies of a set of impulse responses from the experiment are shown in Fig. 7. The control recordings are similar to those shown previously (Fig. 1). In the presence of 3 mmol/l TEA the hump, typically observed in the RA neurons, became apparent and was observed even in responses to small current stimulations. Frequency of the impulse responses were more noisy and considerably larger than those in the control recordings. Lidocaine exposure increased frequency of the impulse responses in general. The increase was apparent in the initial part, and an accelerated decay was observed in the rest of the response. Frequency of the impulse response increased at all stimulation levels when the cell was exposed to *Leiurus quinquestriatus* venom. The multiple decaying components, generating the hump in the impulse frequency curve, disappeared and an apparent noise was observed.

Firing properties of the SA neuron differed in several ways from those of RA neuron. Contrary to the limited firing capacity of the RA neuron, SA neuron was able to convert the current stimulus into impulse frequency for long periods of time. When a super pulse, 30–50 pA larger than the preceding pulse of 5 nA, was introduced a noticeable increase in the impulse frequency was observed (not shown). As shown in Fig. 8 impulse frequency response to a certain current stimulation was not dependent on the previous conditions. If the initial part of the stimulation was not taken into consideration, firing frequency of the receptor neuron was similar whether the neuron was stimulated with a current pulse of 10 nA directly or in

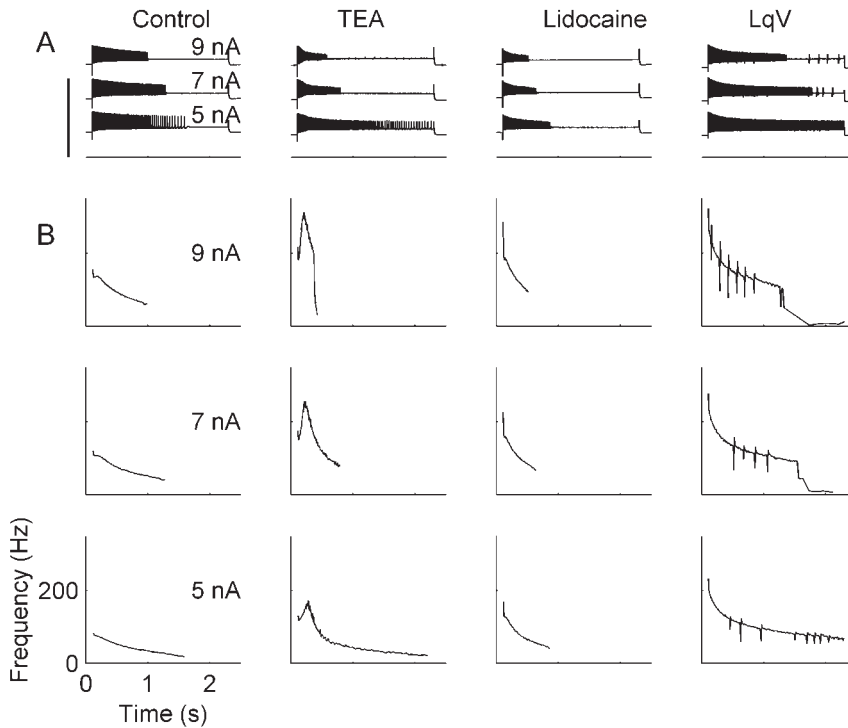


Figure 7. Effects of some chemicals on receptor responses of a rapidly adapting neuron. Neuron is stimulated by constant current injections in control, 3 mmol/l TEA, 1 mmol/l Lidocaine and 10^{-2} mg/ml *Leiurus quinquestriatus* venom (LqV) solutions. The potential (A) and impulse frequency (B) responses at indicated conditions are shown. Time and frequency scale is same in all graphs and the vertical bar in A represents 200 mV.

5 nA steps (Fig. 8A). Further, the initial firing rate, to 5 nA current stimulation, was resumed when the stimulus was stepped down from the 10 nA to 5 nA level (Fig. 8A). As shown in Fig. 8B, a saturating current injection ceased firing. However, the initial firing frequency was achieved by decreasing the current stimulus to the previous level. The SA neuron was capable of resuming the initial firing rate with an error of about -1.6 ± 0.17 Hz ($n = 3$).

Exposing SA neurons to 3 mmol/l TEA or 1 mmol/l Lidocaine decreased the impulse duration to large current stimulations (Fig. 9A). Impulse frequency response increased and had an anomalous waveform when the cell was exposed to TEA. The impulse frequency increased and decreased by 1 mmol/l Lidocaine exposure at small and large current stimulations, respectively. The SA neurons ($n = 4$) either fired spontaneously at a constant rate or in bursts of APs if they were exposed to 5–10 mmol/l Lidocaine (Fig. 9B). The effect was readily removed by washing the Lidocaine away. A spontaneous bursting behaviour was promptly

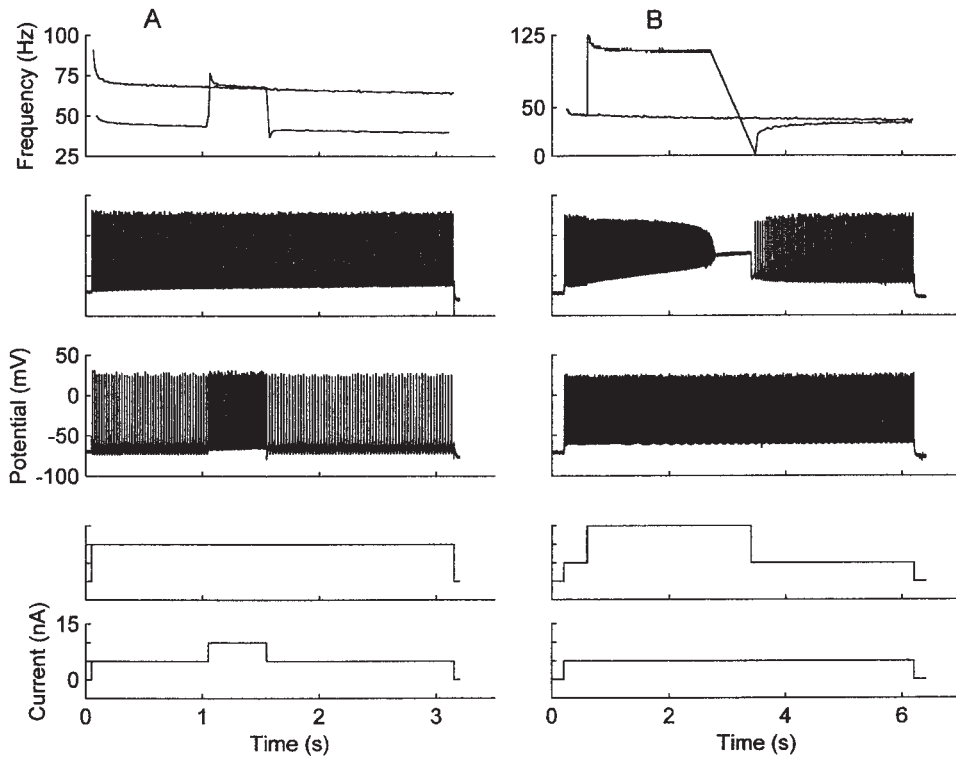


Figure 8. Receptor responses to various current stimulations in the slowly adapting neurons. Neurons are stimulated by the two current pulses displayed at the bottom of each column. Middle traces are the evoked impulse responses and the top traces are superimposed impulse frequency responses. Potential and current scale is the same, time scale in each column is as indicated at the bottom. A and B represent different neurons.

observed when the SA neuron was exposed to 10^{-2} mg/ml *Leiurus quinquestriatus* venom (Fig. 9C).

Fig. 10 shows the impulse and impulse frequency responses to current stimulations recorded in the axon, 1–1.5 mm away from the soma, of the rapidly adapting and the slowly adapting neurons. Pulse trains consisted of two components differing in their adaptive behaviour, firing rate and the amplitude of the individual APs. The components were apparent at large current stimulations. In the RA axon long current stimulations, irrespective of its amplitude, evoked adapting impulse responses (Fig. 10A). In none of the RA axons ($n = 23$) it was possible to induce a non-adapting pulse train. In the SA axons ($n = 12$) non-adapting impulse responses were promptly observed, and only saturating current injections caused adaptation (Fig. 10B,C). In four SA axons spontaneous firing activity was observed.

In both the SA and RA axons the impulse frequency responses were flat for

Table 1. Comparison of the properties of the action potentials in the experimental groups

A		
	AP amplitude	AP duration
Slowly adapting neuron		
Soma (<i>a</i>), <i>n</i> = 25	87.0 ± 1.2 (mV)	2.1 ± 0.1 (ms)
Axon (<i>b</i>), <i>n</i> = 12	75.8 ± 2.2	2.2 ± 0.2
Rapidly adapting neuron		
Soma (<i>c</i>), <i>n</i> = 21	56.2 ± 2.6	2.8 ± 0.4
Axon (<i>d</i>), <i>n</i> = 23	68.0 ± 2.3	1.3 ± 0.1
B		
	AP amplitude	AP duration
<i>p</i> for 1-way ANOVA test (<i>a, b, c, d</i>)	1.1×10^{-16}	3.3×10^{-5}
<i>p</i> for Fischer's <i>t</i> -test		
<i>a</i> vs <i>b</i>	6.9×10^{-4}	0.49
<i>a</i> vs <i>c</i>	9.1×10^{-15}	0.21
<i>a</i> vs <i>d</i>	3.2×10^{-9}	5.1×10^{-5}
<i>b</i> vs <i>c</i>	1.1×10^{-6}	0.26
<i>b</i> vs <i>d</i>	1.4×10^{-2}	6.8×10^{-4}
<i>c</i> vs <i>d</i>	6.8×10^{-5}	3.6×10^{-5}

Amplitude and duration of the action potentials in the experimental groups (*a, b, c, d*) are shown in A (Means ± S.E.M., *n* refers to the number of neurons experimented). Computed frequency distribution values, *p*, by Fischer's *t*-test and one-way ANOVA analysis of the experimental data, are shown in B.

small current injections. However, at large current stimulations, overlapping components caused noise and an anomalous waveform (Fig. 10).

The APs

In four different experimental groups APs were recorded in the soma and the axon, 1–1.5 mm away from cell soma, of the RA and the SA neurons. Quantitative properties of APs are shown in Table 1.

The largest AP amplitude was observed in the soma of the SA neuron (87 ± 1.2 mV), and the smallest amplitude was obtained in the soma of the RA neuron (56.2 ± 2.6). APs in the SA axon (75.8 ± 2.2) were larger than those recorded in the RA axon (68 ± 2.3). Duration of the APs in the RA axon (1.3 ± 0.1 ms) was shorter than the one obtained in the RA soma (2.8 ± 0.4), SA soma (2.1 ± 0.1) and SA axon (2.2 ± 0.2). One-way ANOVA analysis of the data indicated that the amplitude and duration of the APs from the experimental groups were significantly different. Multiple comparison of groups by Fisher's protected *t*-test indicated that amplitude of APs differed significantly when any pair was compared (Table 1B). An identical comparison indicated that only the duration of the APs in the RA axons

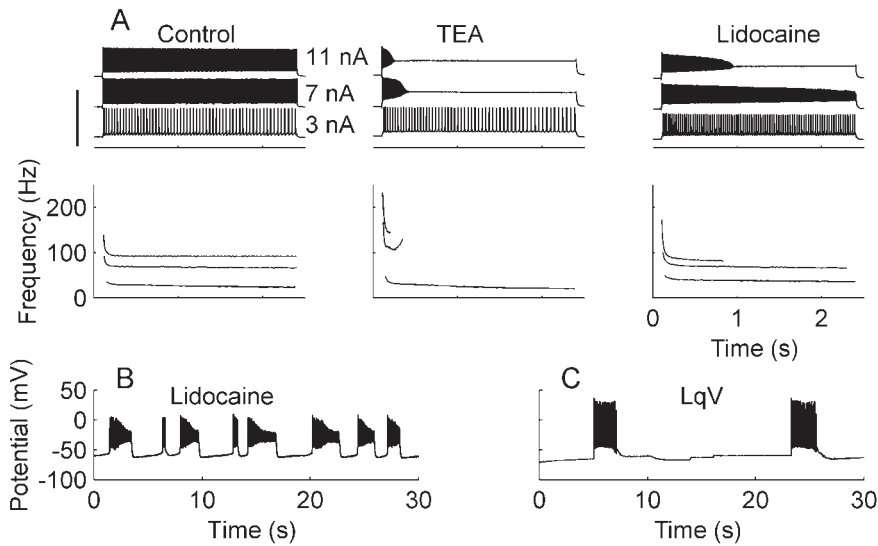


Figure 9. Effects of some chemicals on receptor responses of the slowly adapting neurons. A, the receptor neuron is stimulated by rectangular current injections (3, 7, 11 nA) in control (left column), 3 mmol/l TEA (middle column), 1 mmol/l Lidocaine (right column) solutions. In each column the potential responses (at the top) and the superimposed impulse frequency responses (at the bottom) at indicated conditions are shown. Time and frequency scale is common for the whole A and the vertical bar is 200 mV. Spontaneous firing activity in the presence of 5 mmol/l Lidocaine (B) and 10^{-2} mg/ml *Leirus quinquestriatus* venom (LqV) (C). A, B, C, come from different neurons.

was significantly shorter than that in the other experimental groups (Table 1B).

In another group of experiment ($n = 7$), data were compiled by recording APs both in the axon and in the soma of each SA neuron. Correlation analysis, used to assess the relation between the paired amplitudes of the axonal and the somal APs, indicated that they were not significantly related ($r = 0.57$, $p > 0.05$).

Morphology of the axons

The central extensions from soma of the RA and SA receptor neurons constituted the afferent axons to the ventral ganglia through the dorsal segmental nerve. The dorsal segmental nerve was represented by a single layer of axons covered by some connective tissue. In the majority of the preparations investigated, the RA axon was located laterally in the caudal edge of the segmental nerve. The diameter at about 1–1.5 mm away from the cell soma was $16.6 \pm 0.9 \mu\text{m}$ ($n = 15$). Starting from the axon hillock the SA axon gradually decreased to its smallest diameter within 200–300 μm away from the cell soma. The axonal diameter increased gradually within another 200–300 μm , and was constant at further part of the axon. The SA axon was located adjacently and frequently medially to the RA axon in the

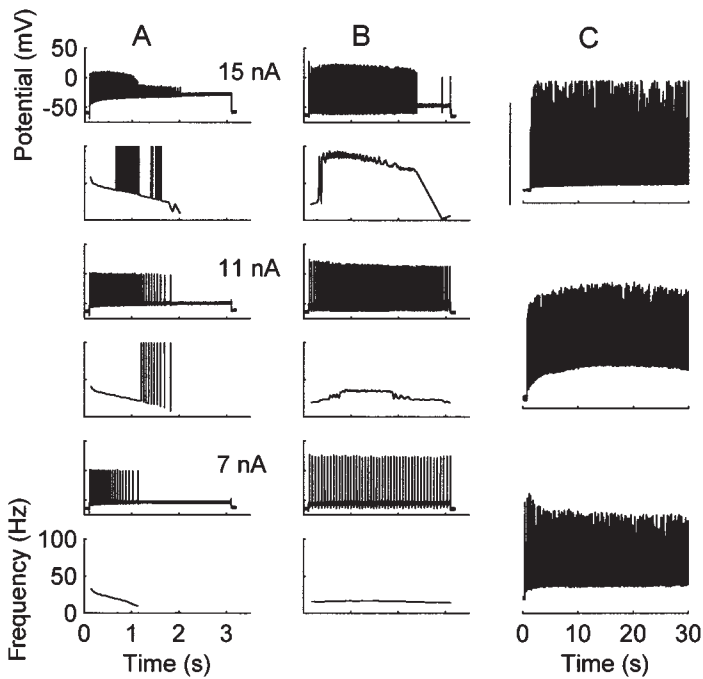


Figure 10. Axonal responses to 7, 11, 15 nA current stimulations in the rapidly (column A) and slowly (column B) adapting axons ~ 1 mm away from neuronal soma. Impulse response to the indicated stimulation level and its frequency curve are shown in consecutive order from top to bottom. Scales are the same. Impulse responses to maintained current stimulation in three different slowly adapting axons are given in column C. Vertical bar represents 75 mV and time scale is at the bottom.

segmental nerve. The SA axon was separated from the RA axon by a single layer of glial cells. The diameter of the SA axon at about 1–1.5 mm away from cell soma was $11.1 \pm 0.6 \mu\text{m}$ ($n = 15$). In all the preparations the diameter of the RA axon was 1.3–2.1 times larger than the diameter of the SA axon.

Discussion

Impulse responses

The SA neuron has a unique ability to code the current intensity into impulse frequency. It is sensitive to current changes as small as 30–50 pA corresponding to opening of some 400–700 mechano-sensitive channels under physiological conditions (Erxleben 1989). It fires at the same frequency irrespective of the previous stimulation conditions if some time is given to achieve a steady level (Fig. 8). Ignoring the initial part, the impulse frequency response to a constant current stimulus is

almost constant (Fig. 1). A similar observation has been reported for the tension responses of the SA receptor muscle (Rydqvist et al. 1990). Thus, it is possible to assume that the SA receptor organ should have been evolved into transducing the maintained length changes in the receptor muscle (Fields 1976).

In the SA neuron, adaptation of the impulse response can only be observed if a large depolarising current, 15–25 nA, is injected (Fig. 8B). Depolarisation block in the encoder membrane is responsible for the adaptation of the impulse responses (Purali 1997; Purali and Rydqvist 1998). However, even under this condition the impulse frequency curve is rather flat. Adaptation at small current injections can only be initiated by some pharmacological interventions (Fig. 9). Blocking the potassium currents by TEA exposure leads to a larger depolarisation amplitude than that which can be achieved by the same current stimulation in the control solution (Fig. 9). Transition of the sodium channels into inactivated state by the excess depolarisation disables generation of the successive APs and causes termination of the impulse responses. The mechanism of the TEA action is an analogy to that of the saturating current injection experiment (Fig. 8B). However, the anomalous shape of the impulse frequency response (Fig. 9) indicates that the firing properties of the SA neuron in the presence of TEA are apparently different from those of a RA neuron under physiological conditions (cf. Fig. 1). If the SA neuron is exposed to 1 mmol/l Lidocaine, a comparable adaptive behaviour is observed when large (11–15 nA) current stimulations are used (Fig. 9A). Lidocaine, a use-dependent blocker of the sodium channels (Hondegheem and Katzung 1984), behaves as an artificial inactivation gate and provides adaptation at large current stimulations when the firing rate (i.e. use of the sodium channels) is frequent. However, increasing Lidocaine concentration further to enable adaptation at small current stimulations leads to unexpected spontaneous firing, and the bursts of APs (Fig. 9B). Considering the available data, a conceivable explanation of the paradoxical effect is not present yet. Perhaps, some further current recording experiments and a detailed modelling of the drug-receptor interactions are required.

Similar to the situation in the SA neuron, it is apparent that the RA neuron is mainly involved in converting the current stimulus into neural codes. The current stimulus under the physiological conditions is the receptor current developing as a response of a receptor to the mechanical stimulus (Rydqvist and Purali 1993). Though both the SA and RA receptors specifically sense the same modality, the RA neuron is capable of transducing the stimulus only for a limited period of time, since impulse response fades away completely at a comparable rapid rate (Fig. 1). The physiological task of the RA neuron is probably limited rather to respond to the rapidly changing features of the stimulus (Fields 1976). Impulse responses to super pulses (Fig. 3A) and, stopping the impulse response to a sudden drop in the stimulus intensity (Fig. 3B) is in support of this idea. Further, the experiments using current ramps indicate that irrespective of its amplitude an adequate ramp rate is required to evoke an AP (Fig. 3C). Present data indicate that the RA neuron may be sort of a rate receptor coding mainly the sudden changes in the stimulus amplitude. The postulate is relevant to a former report that maintained impulse

responses were evoked only by sinusoidal current stimulation (Purali and Rydqvist 1998). It should be pointed out that in the RA neuron presence of impulse activity is related to an increase in stimulus amplitude (Figs. 3 and 5). Thus, unlike to the SA receptor the RA neuron transduces selectively increases in stimulus amplitude.

Considering the fact that receptor current is related to the tension in the receptor muscle (Rydqvist and Purali 1993), firing properties of the RA neuron are compatible with the visco-elastic properties of the receptor muscle (Rydqvist et al. 1994). Tension adaptation is more pronounced in the RA muscle fibre than in the SA one. Thus, the rapidly developing peak tension response may evoke an increasing impulse frequency response during the ramp period while the decay in the tension response during the hold period may facilitate adaptation. Present results obtained using the calculated receptor current confirm the prediction (Fig. 4B). Further, visco-elastic properties of the receptor muscle (Rydqvist et al. 1994) may prevent saturation in the encoder membrane and enable receptor responses to some cumulative stimulations (Fig. 5).

Firing duration in the RA neuron can be modulated by exposing the neuron to some chemicals (Fig. 6). Though firing duration could be increased at some stimulations, the anomalous impulse frequency response (Fig. 7) indicates that a SA mode may not be supplied by exposing the neuron to TEA. Block of the potassium channels and the increase in the input resistance (R_i) of the neuron are the most probable causes of the observed effects. In the presence of 1 mmol/l Lidocaine, both the decrease in firing duration and the accelerated decay in the firing rate are comparable with the established effects of the drug (Hondenghem and Katzung 1984). Such effects of Lidocaine is qualitatively similar in both RA and the SA neurons. However, it should be emphasised that, by increasing the concentration further a spontaneous firing activity can be evoked only in the SA neuron (Fig. 9B). It has been reported that exposing the receptor neuron to *Leiurus quinquestriatus* venom increases the inactivation time constant and shifts the inactivation curve to more positive potential levels (Purali and Rydqvist 1998). In the presence of the venom the sodium channel population is relatively resistant to the inactivation. This effect should be the main cause of the increase in both the firing duration (Fig. 6) and impulse frequency (Fig. 7). The overlapping APs, leading to the apparent noise in the impulse frequency responses (Fig. 7), indicate that in the presence of the venom APs could be initiated in various sites.

In constructing a stimulus-response relationship it is possible to use AP count as an alternative to the impulse frequency measurement when experimenting on SA receptors in general. Fit results obtained by using either AP count ($n = 0.570$, $a = 48/2$, $rv = 0.0079$) or mean impulse frequency ($n = 0.576$, $a = 23.6$, $rv = 0.0080$) response are similar in the SA neuron. However, when RA receptors are experimented, this intervention may lead to errors, since timing information is ignored in the extracted parameter. Adaptation in three of the RA cells displayed in Fig. 2 has resulted in an apparent deviation between the experimental data points and calculated relationship ($rv = 0.0481$). Thus, it may be proposed that the frequency measurement should be superior to the AP count since, it directly

represents a physiological response. However, if the impulse frequency responses are chosen for comparison at a certain moment of the stimulations, timing of the receptor responses limits the comparison to the moments, when receptor responses are not adapted. The mean impulse frequency measurement, used in the present study, is freed from such a limitation which may particularly be important when working with long stimulations. Analysis of the present results indicates that in both RA and SA receptor neurons, impulse frequency responses to constant current stimulations are similar while timing of those responses is apparently different.

Current stimulations evoke pulse trains in both the RA and SA axon (Fig. 10) as observed in the somal recordings. However, unlike the somal recordings, in axonal recordings pulse trains are consisted of two components, differing in their firing properties. This observation indicates that the antidromic and orthodromic spikes are generated at the site of stimulation (Fig. 10). The differences in firing behaviour between components should mainly be related to distance between the current injection site and spike initiating sites. However, a reliable quantitative data could hardly be extracted from the overlapping pulse trains. Thus, only a qualitative comparison of adaptive behaviour of the impulses is possible. The fact that maintained impulse responses could not be evoked in the RA axon indicates that adaptive properties of the RA axon and soma are similar. This, to some extent, is expected since RA soma is not excitable (Purali 1997; Purali and Rydqvist 1998). Thus, the somal recordings are, in fact, a remotely recorded axonal activity. The SA axon has a capacity to initiate maintained pulse trains for long periods of time (Fig. 10C). This is the major difference between the RA and SA axons. However, by using an extracellular stimulation and recording method, Nakajima and Onodera (1969) have reported that beyond the axonal region near the soma, the SA axon lacks the ability to give maintained spike discharges. Though the method used in their study is very creative, however, it required a complete dissection of the axons from each other which might lead to the discrepancy between the results.

Action potential

Duration of the AP is significantly shorter in the axon of the RA neuron as compared to that from the other experimental groups (Table 1). Somal recordings in the RA neuron are, in fact, the passively spreading axonal APs (Purali 1997; Purali and Rydqvist 1998). Thus, antidromic electrotonic spread may be the main cause of both the longer duration and the lower amplitude. Besides, smaller amplitude of the somal AP may indirectly contribute to the elongation by activating less potassium current, taking part in termination of the signal.

However, the arguments above may not be relevant when comparing the AP duration in the RA axon to that in the soma and the axon of the SA neuron (Table 1). It is apparent that the sodium currents are present in both the soma and axon of the SA neuron (Purali 1997; Purali and Rydqvist 1998). Thus, present results do not supply sufficient information to convincingly explain the difference. Perhaps, some further experiments in those neuronal parts are required.

An apparent difference between the experimental groups is observed when the amplitude of the APs is compared. The statistical analysis indicates that none of the paired results are similar (Table 1). The main discussion below, about the differences in the AP amplitude, is focused on the geometry of the neurons and the properties of sodium currents. The possible effects of the potassium currents are not considered due to the relatively slow time course and the similarity of the macroscopic currents in both neurons (Rydqvist and Purali 1991; Purali and Rydqvist 1992).

In the RA neuron, the significantly lower amplitude of the somal recordings as compared to that of the axonal ones is relevant to former data by Purali and Rydqvist (1998). Though a controversial observation has been reported by Eyzaguirre and Kuffler (1955), this should be ignored since neither a cumulative result nor a statistical evaluation has been presented. The difference between the axonal and somal recordings could conclusively be explained by the absence of sodium channels in the soma of the RA neuron (Purali 1997; Purali and Rydqvist 1998). The apparent increase in the AP amplitude (Table 1) as the recording electrode was moved towards the sites with sodium channels, i.e. axon, is a direct support for the interpretation (Purali and Rydqvist 1998).

The AP amplitude in the RA neuron is smaller than that recorded in the soma and the axon of the SA neuron (Table 1). The SA axon is 1.3–2.1 fold thinner in diameter as compared to RA axon. Assuming an identical density of a sodium channel population, geometrical variations defining the passive properties might be responsible for the difference between axonal APs. However, such an argument fails to explain why the somal AP in the SA neuron has the largest amplitude. Should the sodium channel density in the SA soma be identical to that in both axons then, due to the physical properties of the soma a comparatively smaller amplitude would be expected. Alternatively, it might be proposed that the sodium channels might be more densely distributed in the soma of the SA neuron than the other recording sites. As a matter of fact, according to the Hodgkin and Huxley (1952) equations, AP amplitude increases with the sodium channel conductance (g_{Na^+}). However, increase in g_{Na^+} is expected to decrease the firing threshold and increase the impulse frequency. As reported in the former studies the threshold level is similar in both the RA and SA neuronal soma (Eyzaguirre and Kuffler 1955; Nakajima and Onodera 1969; Purali and Rydqvist 1998) and receptor neurons have similar firing frequencies (Fig. 2). Thus, some other factors should have been involved.

Purali and Rydqvist (1998) have reported that in the SA neuron voltage clamp recordings indicated two macroscopic sodium current components. One of the components, which is present only in the SA neuron, is activated at more positive potential levels and is more resistant to inactivation. Thus, it is conceivable to propose that possible differences in the axonal and somal sodium currents might contribute to the differences in the AP and impulse responses (Purali 1997). The interpretation is supported by the observation that slowing down the sodium channel inactivation, by scorpion venom exposure, increases AP amplitude and firing

duration considerably (Purali and Rydqvist 1998, Fig. 6). Further, the amplitudes of the paired APs from the axon and the soma of the same SA neuron are not related. It implies that, the biological systems generating the axonal and somal APs may be independent mechanisms.

Analysis of present data supports the former postulate that the observed differences in the firing properties of the receptor neurons stem from the differences in the active and the passive properties of the neurons (Purali 1997). However, the hypothesis needs to be further experimented in a mathematical model considering the geometrical properties and, passive and active components of the receptor neurons.

Acknowledgements. I would like to thank Drs. S. Yagcioglu and R. Soylu for help in programming. This study was supported by Hacettepe University Research Foundation and The Scientific and Technical Research Council of Turkey.

References

- Alexandrowicz J. S. (1951): Muscle receptor organs in the abdomen of *Homarus vulgaris* and *Palinurus vulgaris*. *Q. J. Microsc. Sci.* **92**, 163—200
- Brown M. C., Stein R. B. (1966): Quantitative studies on the slowly adapting stretch receptor of the crayfish. *Kybernetik*. **3**, 175—85
- Carmer S. G., Swanson M. R. (1973): An evaluation of ten multiple comparison procedures Monte Carlo methods. *J. Am. Stat. Assoc.* **68**, 66—74
- Chaplain R. A., Michaelis B., Coenen R. (1971): Systems analysis of biological receptors. A quantitative description of the input-output characteristics of the slowly adapting stretch receptor of the crayfish. *Kybernetik*. **9**, 85—95
- Erxleben C. (1989): Stretch-activated current through single ion channels in the abdominal stretch receptor organ of the crayfish. *J. Gen. Physiol.* **94**, 1071—1083
- Eyzaguirre C., Kuffler S. W. (1955): Further study of soma, dendrite, and axon excitation in single neurons. *J. Gen. Physiol.* **39**, 121—153
- Fields H. L. (1976): Crustacean abdominal and thoracic muscle receptor organs. In: *Structure and Function of Proprioceptors in the Invertebrates* (Ed. P. J. Mill), pp. 65—114, Chapman & Hall, New York and London
- Guharay F., Sachs F. (1984): Stretch-activated single ion channel currents in tissue-cultured embryonic chick skeletal muscle. *J. Physiol.* **169**, 424—430
- van Harreveld A. (1936): A physiological solution for freshwater crustaceans. *Proc. Soc. Exp. Biol.* **34**, 428—432
- Hodgkin A. L., Huxley A. F. (1952): A quantitative description of membrane currents and its application to conduction and excitation in nerve. *J. Physiol.* **117**, 500—544
- Hondeghem L. M., Katzung B. G. (1984): Antiarrhythmic agents: the modulated receptor mechanism of action of sodium and calcium channel-blocking drugs. *Annu. Rev. Pharmacol. Toxicol.* **24**, 387—423
- Nakajima S., Onodera K. (1969): Membrane properties of the stretch receptor neurones of crayfish with particular reference to mechanisms of sensory adaptation. *J. Physiol.* **200**, 161—185
- Purali N. (1997): Mechanism of adaptation in a mechanoreceptor. A study of mechanical and ionic factors in the crayfish stretch receptors. *Repro Print AB, Stockholm*

- Purali N., Rydqvist B. (1992): Block of potassium outward currents in the crayfish stretch receptor neurons by 4-aminopyridine, tetraethylammonium chloride and some other chemical substances. *Acta. Physiol. Scand.* **146**, 67—77
- Purali N., Rydqvist B. (1998): Action potential and sodium current in the stretch receptor neurons in the crayfish. *J. Neurophysiol.* **80**, 2121—2132
- Rydqvist B., Purali N. (1991): Potential-dependent potassium currents in the rapidly adapting stretch receptor neuron of the crayfish. *Acta. Physiol. Scand.* **142**, 67—76
- Rydqvist B., Purali N. (1993): Transducer properties of the rapidly adapting stretch receptor neuron in the crayfish (*Pacifastacus leniusculus*). *J. Physiol.* **469**, 193—211
- Rydqvist B., Swerup C., Lannergren J. (1990): Visco-elastic properties of the slowly adapting stretch receptor muscle of the crayfish. *Acta. Physiol. Scand.* **139**, 519—527
- Rydqvist B., Purali N., Lannergren J. (1994): Visco-elastic properties of the rapidly adapting stretch receptor muscle of the crayfish. *Acta. Physiol. Scand.* **150**, 151—159
- Smith T. C., Lecar H., Redman S. J., Cage P. W. (1985): Voltage and patch clamping with microelectrodes. pp. 24—42, Williams and Wilkins, Baltimore, VA, U.S.A.
- Swerup C., Rydqvist B. (1992): The abdominal stretch receptor organ of the crayfish. *Comp. Biochem. Physiol.* **103**, A423—431
- Swerup C., Rydqvist B. (1996): A mathematical model of the crustacean stretch receptor neuron. Biomechanics of the receptor muscle, mechanosensitive ion channels, and mechanotransducer properties. *J. Neurophysiol.* **76**, 2211—2220
- Steevens S. S. (1957): On the psychophysical law. *Psychol. Rev.* **64**, 153—181
- Terzuolo C. A., Washizu Y. (1962): Relation between stimulus strength, generator potential and impulse frequency in stretch receptor of crustacea. *J. Neurophysiol.* **25**, 56—66
- Welowitz J., Even R. B., Cohen J. (1982): *Introductory Statistics for the Behavioral Sciences*. pp. 237—255, Harcourt Brace Jovanovich Inc., Florida, U.S.A.
- Wiersma C. A., Furshpan E., Florey E. (1953): Physiological and pharmacological observations on muscle receptor organs of the crayfish, *Cambarus clarkii Girard*. *J. Exp. Biol.* **30**, 136—50

Final version accepted: January 3, 2002